BIOLOGICAL SCIENCES: Evolution

Ecological causes of uneven diversification and richness in the mammal tree of life

Short title: Ecological causes of diversification in mammals

Nathan S. Upham[1*], Jacob A. Esselstyn[2], and Walter Jetz[1*]

Author affiliations: [1]Department of Ecology & Evolutionary Biology, Yale University, New Haven, CT 06511 USA. [2]Department of Biological Sciences and Museum of Natural Science, Louisiana State University, Baton Rouge, LA 70803 USA.

*Corresponding author: Nathan S. Upham; address: 165 Prospect St., OML 122, New Haven, CT 06511 USA; phone: 773-263-1533; email: nathan.upham@yale.edu.

Abstract

The uneven distribution of species in the tree of life is rooted in unequal speciation and extinction among groups. Yet the causes of differential diversification are little known despite their relevance for sustaining biodiversity into the future. Here we investigate rates of species diversification across extant Mammalia, a compelling system that includes our own closest relatives. We develop a new phylogeny of nearly all ~6000 species using a 31-gene supermatrix and fossil node- and tip-dating approaches to establish a robust evolutionary timescale for mammals. Our findings link the causes of uneven modern species richness with ecologically-driven variation in diversification rates, including 24 detected rate shifts. Speciation rates are a stronger predictor of among-clade richness than clade age, countering claims of clock-like speciation in large phylogenies. Surprisingly, rate heterogeneity in recent radiations shows limited association with latitude, despite the well-known richness increase toward the equator. Instead, we find a deeper-time association where clades of high-latitude species have the highest speciation rates, suggesting that species durations are shorter outside than inside the tropics. At shallower timescales (i.e., young clades), diurnality and low vagility are both linked to greater speciation rates and extant richness. High turnover among small-ranged allopatric species may erase the signal of vagility in older clades, while diurnality may adaptively reduce competition and extinction. These findings highlight the underappreciated joint roles of ephemeral (turnover-based) and adaptive (persistence-based) diversification processes, which manifest as speciation gradients in recent and more ancient radiations to explain the evolution of mammal diversity.

Keywords

Phylogenetics, macroevolution, dispersal, mass extinction

Significance statement

The over 6000 living species in the mammalian tree of life are distributed unevenly among branches so that similarly aged groups sometimes differ many fold in species richness (e.g., ~2500 rodent species versus 8 pangolins). Why differential bursts of species diversification occur, and how long they persist, has implications for sustaining biodiversity. Here we develop a robust evolutionary timescale for most extant species, recovering signatures of rate-variable diversification linked to ecological factors. Mammals with low dispersal or that are day-active show the fastest recent diversification, consistent with mechanisms of allopatric speciation and ecological opportunity, respectively. Speciation rates are surprisingly faster in extra-tropical than tropical lineages, suggesting that longer species durations for tropical lineages underpin the latitudinal diversity gradient in mammals.

\body

Introduction

Branches in the mammal tree of life range from mega-diverse rodents and bats to similarly old, yet species-poor, groups like treeshrews and pangolins (stem ages all ~60-70 million years ago [Ma]). Questioning why some evolutionary groups are more speciose than others traces to the classic 'hollow curve' observation of Willis (1), which was formalized for phylogenetic tree shape as unevenness (or imbalance) (2). Uneven species richness implies uneven net diversification (speciation – extinction), but whether speciose clades usually derive from faster rates or older ages is controversial (2–4). Similarly debated are the causal roles of environmental factors (3, 5–7) or intrinsic traits of species (8, 9) as determinants of rate-variable diversification. Recently, analytical advances in identifying macroevolutionary rate regimes (10) and species-level rate variation at the instantaneous present (e.g., the tip DR metric (11, 12)) have uncovered gradients of higher speciation rates with latitude (13–15) and elevation (7). Ephemeral speciation processes (16) appear to underlie these dynamics, where unstable environments produce many short-lived species via high turnover (speciation + extinction). In contrast, adaptive processes that involve accessing novel ecospace are expected to decrease extinction rates (6, 17, 18), so that species accumulate via persistence rather than turnover. If nascent allopatric species form regularly (19), then identifying which factors cause them to persist or go extinct (e.g., habitat seasonality, dispersal ability, niche adaptations; (7, 13, 14, 16, 19–21)) is central to understanding why evolutionary tree shapes and geographic diversity are uneven. The challenge to reconstructing species birth and death across Mammalia is that a robust evolutionary timescale is required for among-clade tests of rate variation to be meaningful.

Until now, the species-level phylogenies of mammals have been inadequate for the task of understanding macroevolutionary tree shape. Parsimony supertrees (22) were first

72 implemented on large scales across Mammalia (Bininda-Emonds et al. (23) and its updates (24,
73 25)). However, supertree methods add artifacts of short branch lengths when merged source trees
74 disagree (e.g., >50% of nodes in Bininda-Emonds et al. (23)), and are thus biased toward
75 inferences of rapid radiation at regions of the tree with the greatest phylogenetic uncertainty. For
76 example, a series of polytomies in rodents and bats were inferred as an ~30-Ma pulse of tree-
77 wide diversification ((26); *SI Appendix*, Fig. S14 for a comparison of tree shapes). Despite this
78 issue, supertrees continue to be a popular choice for large-scale phylogenetic inference and tests
79 of diversification rate hypotheses (e.g., 27, 28). Herein, we abandon the supertree paradigm,
80 using instead a single DNA supermatrix to improve upon the Bayesian backbone-and-patch
81 approach developed in birds (11), squamates (29), and amphibians (30).
82 Our mammal tree (Fig. 1) includes 5,804 extant and 107 recently extinct species in a
83 posterior distribution of 10,000 trees, integrates age and topological uncertainty, and incorporates
84 1,813 DNA-lacking species using probabilistic constraints. It thereby offers a species-level
85 phylogeny with all branches estimated under a unified birth-death model (available at
86 vertlife.org). Trees are built using: (i) an updated taxonomy; (ii) a newly assembled 31-gene
87 supermatrix; and (iii) the backbone-and-patch framework, which estimates the phylogenies of 28
88 mammal subclades (identified in a global DNA tree) with relative branch lengths, re-scales the
89 branches to corresponding divergence times in fossil-calibrated backbones, and grafts each
90 subclade to the backbone (Fig. 2; *Methods*, *SI Appendix*, Datasets S1-S6). We developed four
91 posterior sets of Mammalia-wide trees based on node- or tip-dated backbones (31, 32) and the
92 inclusion or exclusion of DNA-lacking species. Analyzing samples of trees from each set yields
93 some variation in node ages, but consistent results across all comparative analyses (*SI Appendix*,
94 Fig. S9-11, S21-S22).

95 Here we use this novel phylogenetic framework to investigate the potential extrinsic and
96 intrinsic causes of uneven diversification in mammals, including whether evolutionary rate
97 processes are recorded differently in recent radiations vs. older clades where extinction is more
98 likely to have pruned lineages from trees of extant species (33, 34).

99 **Results and Discussion**

100 **Tree-wide and among-clade tempo of lineage diversification.** The absolute and
101 relative timings of mammal diversification are debated (23, 35), with particular controversies
102 around whether early placentals diverged before, after, or during the Cretaceous-Paleogene (K-
103 Pg) mass extinction event, 66 Ma (short fuse, long fuse, or explosive models, respectively (36)).
104 We estimate the age of crown Placentalia at 92 Ma (95% confidence interval [CI] of 77, 105
105 using node-dating; tip-dating yielded mostly similar results, *SI Appendix*, Fig. S9). The first four
106 placental divergences unambiguously preceded the K-Pg (Fig. 3a; filled circles), followed by the
107 next 21 divergences with CIs that overlap the K-Pg (Fig. 3a–b). We find a Cretaceous "fuse" of
108 ~25-Ma between the radiation of crown Placentalia and nine of 18 crown orders (*SI Appendix*,
109 Table S6), in line with some estimates (35, 37), but longer than others (e.g., (23)). The burst of
110 tree-wide lineage turnover we recover near the K-Pg (visual anomalies in speciation and
111 extinction rates; Fig. 3c) is remarkable for matching concurrent fossil evidence for pulses of
112 origination and extinction (36, 38, 39) (Fig. 3d). Despite spatiotemporal biases in fossil
113 preservation (40, 41) and extant phylogeny reconstruction (33), corroboration between these
114 genetic and fossil data suggests they reflect genuine dynamics in mammalian evolution (42).

115 We recover at least 24 lineage-specific shifts in net diversification rates (Fig. 1, 3c, e; *SI*
116 *Appendix*, Table S8), the earliest of which occurs in either crown Placentalia (1.1x higher than
117 the Mammalia-wide median rate of 0.138 species/lineage/Ma) or Boreoeutheria (1.6x, node C in

118 Fig. 1). These shifts involve 18 different lineages and are all positive, except a rate decrease
119 uncovered for the primate clade of lemurs, lorises, and galagos (Strepsirrhini; node O). The two
120 largest rate increases (4.0x and 3.2x) occurred in the last 10 Ma: the gopher-like tuco-tucos of
121 South America (*Ctenomys*, node Q), and the Indo-Pacific flying foxes (*Pteropus*, node J).
122 Overall, rate increases near the present tend to be particularly high, with a 2.2x mean in the
123 Miocene versus 1.3x in each the Oligocene and Eocene (Fig. 3c; df=2, F=7.772, P=0.003), which
124 corroborates the expectation for extinctions deeper in the tree (e.g., (38)) to have reduced our
125 ability to detect more ancient shifts (33, 43). Different to the explosive model (36), no lineage-
126 specific rate shifts implicate the K-Pg in promoting radiations, either preceding the event
127 (Placentalia) or occurring later (Fig. 3c, e). Notably, we record the highest probability of tree-
128 wide rate increases ~15 Ma (*SI Appendix*, Fig. S15c and d), in contrast to previous results for rate
129 decreases ~8 and ~3 Ma in mammals (23, 26).

130 **Within-clade tempo of lineage diversification.** The timings of radiation we recover
131 emphasize that the majority of mammalian diversification in extant lineages occurred during the
132 last ~50 Ma (Fig. 1, 3). Environmental changes during this period are posited to have broadly
133 changed the biosphere (3, 44), with potential imprints on phylogenies as temporal variation in
134 diversification rates (4–6, 42). We predicted that species-rich clades would display stronger
135 signatures than depauperate clades of rate-variable (RV) diversification if RV processes were
136 predominant, since the likelihood of rare events (within-clade shifts in speciation or extinction)
137 and our statistical power to detect them should increase with clade size. We find that models of
138 RV diversification (42) were favored over rate-constant (RC) models (33) for five out of 12
139 placental subclades tested (Fig. 3f; *SI Appendix*, Table S9). The strongest RV signal is in the
140 speciose mouse-related clade of rodents, along with shrews and catarrhine primates and

141 matching observed rate shifts (clades 46, 31, and 42; Fig 1, 3e–f). The cow- and whale-related
142 clades of artiodactyls also have strong RV signatures (Fig. 3e), concordant with previous
143 suggestions (e.g., (42, 43)).

144 As an additional, more sensitive, test we use clade-wide distributions of tip-level (i.e.,
145 species') diversification rates (tip DR (11)) to capture the within-clade rate heterogeneity arising
146 from RV processes (Fig. 3f). We find the overall-highest tip DRs in simian primates (clades 42–
147 43), including the human genus *Homo* (80th percentile, median 0.321 species/lineage/Ma; *H.*
148 *sapiens* and three extinct species) and Indomalayan lutung monkeys (95th percentile, 0.419,
149 *Trachypithecus*), while the distinctive aardvark and platypus have the lowest tip DRs (clades 1,
150 14; Fig. 1). Broadly, we recognize substantial heterogeneity in tip DR across the mammal tree,
151 sometimes with a few high-tip-DR species nested together with low-tip-DR species (Fig. 1),
152 resulting in long right-side tails in the tip DR distributions (positive skew, e.g., clades 38 and 44
153 in Fig. 1, 3f). We find that tip DR skew measures aspects of within-clade rate variation otherwise
154 uncaptured by birth-death models (*SI Appendix*, Table S10).

155 **Time and ecology relative to clade species richness.** The relative importance of clade
156 ages (time) versus rates of speciation and extinction (whether stochastic or ecologically driven)
157 as an explanation of extant diversity levels is a matter of intense debate in mammals (5, 6, 45, 8)
158 and other taxa (19, 46, 28, 47). Past efforts to separate these hypotheses have focused on named
159 clades (e.g., (4)), which are biased by subjective delineation and often vast age differences
160 (mammal families range 3.8–59.0 Ma in mean crown ages; *SI Appendix*, Dataset S7). To avoid
161 this bias, we sliced phylogenies at five-million-year intervals and took the tipward clades as
162 objective units for analysis (Fig. 4a; *SI Appendix*, Fig. S5). Time-sliced clades thus account for
163 the 'pull of the present' in modern trees (48) by analyzing successive levels of rootward

164 covariance among clade crown age, species richness, tip DR mean and skew, and mean
165 ecological traits. If time-constant rates predominate (28, 46, 49), crown ages will explain most of
166 the among-clade variation in species richness. In contrast, if rate variation is strong, as we
167 already recognized for some nodes and named clades (Fig. 3) and expect from varying ecological
168 regimes (2, 5, 6, 19), diversification rates will have the greater explanatory power.

169 We find that clade age and richness are positively correlated—yet significantly less so
170 than the unique effects of tip DR mean and skew on richness (Fig. 4, multivariate PGLS; *SI*
171 *Appendix*, Fig. S18 for univariate and taxon-based results). Critically, clade tip DR mean has
172 stronger effects on richness than expected from simulated RC trees containing only stochastic
173 rate variation (Fig. 4c). Clade tip DR skew is also significant, especially so at deeper time slices
174 (Fig. 4d), confirming that single speed-ups in diversification within a clade (e.g., due to
175 ecological opportunity for one lineage (6, 17)) can drive much of its overall species richness
176 today. These analyses support arguments that ecology is a greater macroevolutionary force than
177 time (47), yet obviously both contribute to richness (adjusted-R^2: 0.88 full model versus 0.26
178 with crown age only, means of 100-tree PGLS among 35-Ma clades). Jointly analyzing richness
179 determinants in time-sliced clades offers an objective way to assess age and rate effects that, in
180 turn, enables tests for ecological drivers of rate variation.

181 **Linking ecology to uneven diversification and richness.** Vagility, latitude, and
182 diurnality are among the key purported causes of variation in mammalian species richness (3, 5,
183 6, 50). Species vagility, through its effect on gene-flow patterns (19, 51), has been posited as
184 inversely related to the probability and scale of geographic isolation, and hence allopatric
185 speciation (21, 52). We performed phylogenetic path analysis (53) to assess the indirect effects
186 of these ecological factors on mammalian richness via their impact on the joint, yet unequal,

187 contributions of rates and ages to extant species numbers (Fig. 5, *Methods*, *SI Appendix*, Fig. S8).
188 Here, the time-sliced clades allow us to distinguish trait-rate dynamics that are localized near the
189 species level (if traits drive ephemeral speciation (16) or if they evolved very recently) from
190 those that occur deeper in the tree and persist (if traits evolved anciently and did not affect
191 extinction rates). We find that at the species level, and especially in herbivores and carnivores,
192 low-vagility mammals have higher tip DRs (Fig. 5a; ecological trait ~ rate PGLS (8)). Effects of
193 vagility on clade tip DR mean are weakened toward deeper time slices, where they are instead
194 recorded on tip DR skew (Fig. 5b). We interpret these short-lived effects of vagility on tip DR
195 mean as consistent with expectations that nascent allospecies are produced at a high rate, but are
196 ephemeral, going extinct before their peripheral isolate can expand (16, 19, 52). While the nearly
197 20% of mammal species endemic to islands complicates our allometric estimate of species
198 vagility (Fig. S9), we note that the ~10-million-year 'threshold' whereby low-vagility lineages
199 find an adaptive zone, evolve greater vagility, or vanish is robust to multiple sensitivity tests (*SI*
200 *Appendix*, Fig. S21-S22). The influence of vagility on diversification, however, might not be
201 linear (e.g., humped (19) or sigmoidal (21)).
202 Latitude, through strong covariation with environmental conditions and species richness,
203 is considered to represent key mechanisms behind cross-taxon disparities in richness (3, 13). But
204 recent evidence casts doubt on this presumed negative association between latitude and
205 diversification rates (11, 13, 14). Here we find that there is no effect of absolute latitude on tip
206 DR at the species level (Fig. 5a). Instead, strong positive associations with latitude arise at
207 deeper time slices, but without corresponding effects on skew (Fig. 5b). Similarly weak latitude-
208 to-rate effects in young clades and species of birds (11, 13, 14) appear to emphasize the impact
209 on species turnover cycles of temperate climatic instability, seasonality, and expansion of new

habitats. We suggest that the traditionally invoked tropical 'cradle' (higher speciation) and 'museum' (lower extinction (3)) should re-focus upon the *turnover ratio* of those processes, testing whether extratropical species are 'cycled' faster than tropical species and, if so, relative to which biogeographic processes. Extratropical lineages may not cycle fully, but instead persist through climatic oscillations in glacial refugia (54). The Eocene-Oligocene transition (~34 Ma) from tropical to temperate habitats (3) would then have initiated converse latitudinal gradients in species turnover and richness, although North American mammal fossils suggests a steeper richness gradient beginning ~15 Ma (55).

Diurnality is a core behavioral-physiological trait tied to temporal niche innovation (50) and the associated potential for adaptive diversification. We find that repeated origins of daytime activity since the late Eocene (~35 Ma (50, 56)) are associated with faster species diversification, both at the present (Fig. 5a) and among 10-Ma time-sliced clades (Fig. 4b). Lineage-specific rate increases also reflect signatures of greater diurnal activity on diversification (*SI Appendix*, Fig. S17a). These results affirm the importance of diurnality (56) in the context of other drivers of rate variation (vagility and latitude), placing previous findings of rapid diversification in diurnal lineages of primates (57) in a broader context. Results for 30- and 50-Ma clades appear to be confounded with nocturnal ancestors, including inverse effects on tip DR skew (Fig. 5b), which is consistent with diurnality evolving well after a "nocturnal bottleneck" among K-Pg-surviving mammals (50). In contrast to vagility and latitude, we posit that greater daytime activity is an example where adaptive divergence in niche traits has decreased extinction rates via competitive release (17), and therefore led to greater persistence and species richness in diurnal lineages.

Conclusions. Our novel, time-calibrated phylogenetic framework addressing all extant and described species of mammals puts a focus on ecological drivers of diversification. Rate-

shifted clades have disparate ecological characteristics (*SI Appendix*, Fig. S17e), suggesting that lineage-specific events have fostered mammalian radiations. Nevertheless, we detect cross-clade signatures of intrinsic (vagility, activity pattern) and extrinsic (latitude) factors driving aspects of diversification at nested phylogenetic levels. We hypothesize that two main processes are at work. First, turnover-mediated diversification is acting on short timescales due to geographic isolation among low-vagility species, and on longer timescales due to the dynamics of extratropical climates. Second, persistence-mediated diversification is demonstrated for diurnal lineages and related more generally to adaptations (or stable habitats) resulting in lower extinction rates. Traversing between these processes may be possible if otherwise ephemeral allospecies can enter novel regions of the phenotype-to-environment landscape, either via niche evolution or extrinsic opportunity (6, 16, 17, 52), to then continue diversifying with lower extinction risk. Overall, we show that ecological factors are influencing diversification rates, but the effects manifest at different hierarchical levels of the tree of extant mammals. Geologically recent processes associated with species turnover or adaptation are not yet studied for most of life, but our results in mammals suggest that gradients in these novelty-originating processes have ecological causes relevant to the capacity for future biodiversification.

Methods

***Building new species-level trees for extant Mammalia* – Overview.** We reconstructed the evolutionary history of extant Mammalia aiming to maximize the accuracy and comparability of temporal information (branch lengths) across lineages in a posterior set of time-calibrated phylogenies. Trees were built using a multi-step strategy (Fig. 2) designed to: (i) sample and vet available DNA sequences for extant and recently extinct species into a 31-gene supermatrix; (ii) use an updated taxonomy accounting for 367 new species and 76 genus transfers (5,911 total species; *SI Appendix*, Table S2 and Dataset S2); (iii) estimate a global maximum likelihood (ML) tree for 4,098 species in the DNA supermatrix to inform taxonomic constraints (*SI Appendix*, Dataset S3); (iv) include species unsampled for DNA within the Bayesian phylogenetic analyses (PASTIS completion (58)); and (v) integrate fossil data at nodes and tips to compare methods of calibrating backbone divergence times in mammals. We modified the backbone-and-patch analysis framework (11) to estimate the relative-time phylogenies of 28 non-overlapping subclades of mammals, called "patches" (identified in the global ML tree; Table S5 and Dataset S3). We then re-scaled branches to corresponding divergence times in fossil-calibrated backbones, and grafted the subclade patches to backbones to form Mammalia-wide trees (*SI Appendix*, Fig. S1-S3). We compared trees built using node-dated backbones (17 fossil calibrations (31)) and tip-dated backbones (matrix of modern and Mesozoic mammals (32)), which yielded broadly similar ages (*SI Appendix*, Fig. S9-S11). Strict topology constraints from the global ML tree were used in the 10,000 taxonomically completed trees (5911 species, 'TopoCons') while the DNA-only trees were estimated without topology constraints (4098 species, 'TopoFree').

DNA gathering pipeline. We used the BLAST algorithm (Basic Local Alignment Search Tool (59)) to efficiently query a local copy of NCBI's nucleotide (nt) database, targeting 31 gene fragments (*SI Appendix*, Table S1) commonly sampled among mammals. Meredith et al. (35) was our starting point since their matrix included most extant families for 22 exons and 5 non-coding regions. We further targeted four protein-coding mitochondrial genes to maximize species-level sampling. For each gene, we used a set of pre-vetted sequences or 'baits' as queries for extracting homologous gene fragments from the NCBI database using the "blastn" executable (BLAST+ version 2.2.31) and the XML2 output format to assign taxonomic information for subsequent parsing.

Synonym resolving and master taxonomy for this study. The NCBI taxonomy of our genetic data contained many synonyms that required matching to accepted mammalian species prior to analysis. We based this matchup on a synonym list compiled from Catalogue of Life, MSW3 (60), and IUCN (total of 195,562 unique equivalencies; updated from Meyer et al. (61)). This procedure yielded direct matches for 75% of the NCBI names from our BLAST search. We matched an additional 765 names via manual reference to the literature and identified 1273 species synonyms to yield a list of 4,217 accepted species with ≥1 sampled gene for subsequent error-checking. This taxonomic matchup also produced a master taxonomy of 5911 mammalian species for this study, of which 5,804 species are considered extant (*SI Appendix,* Table S2). The Mammal Diversity Database (62, 63) (mammaldiversity.org) was an outgrowth of our project, and continues to update mammalian taxonomy as new literature is published.

DNA sequence error-checking and alignment. We used an iterative per-gene approach to clean annotation errors in NCBI, as follows: (i) sequence alignment, (ii) gene-tree construction (RAxML v.8.2.3 (64)), and (iii) error-checking for stop codons and insufficient alignment

294 overlap (Fig. 2a). In total, our error-checking steps excluded 1618 sequences across all genes
295 (i.e., 7.2% of the 22,504 individual DNA sequences; *SI Appendix*, Table S1 and S3)
296 corresponding to 119 species, and yielding 4098 species with ≥1 gene fragment validated in the
297 final 31-gene matrix (Dataset S1 lists excluded sequences).

298 **Global DNA-only ML tree.** Phylogenetic analysis of the 4098-species DNA matrix was
299 first performed in RAxML with the goal to identify the single best-supported topology for global
300 mammals (*SI Appendix*, Table S4, Dataset S3). The supermatrix of 39,099 base pairs (bp) was
301 11.9% complete in terms of ungapped sites, which was a level of missing data not expected to
302 confound phylogeny estimation (65, 66).

303 **Patch subclades and PASTIS completion of missing species.** Examination of well-
304 supported nodes (>75% bootstrap support) in the global ML tree informed our division of the
305 mammalian phylogeny into 28 patch subclades (11). Delimiting patches was an essential step for
306 conducting Bayesian analyses on manageable tree sizes given co-estimation upon 1000 or more
307 species exceeds current computational limits (*SI Appendix*, Fig. S2, Table S5). Taxonomic
308 constraints for MrBayes v.3.2.6 (67) were formed with the R package PASTIS (58), reducing the
309 potential for human error while identifying non-monophyletic genera in the global ML tree (see
310 Dataset S4). Completed species' branch lengths were drawn from the same birth-death
311 distribution as the rest of the patch clade, tending PASTIS completions conservatively to rate-
312 constant processes while preserving the taxonomically expected tree shape (11, 58).

313 **Fossil-dated backbone trees.** Two backbones were constructed: (i) node-dating (ND),
314 using 17 fossil calibrations from Benton et al. (31), as augmented by Philips (68); and (ii) tip-
315 dating (fossilized birth-death, FBD (69)), using the morphological data set of Zhou et al. (32)
316 trimmed to 76 fossil and 22 extant taxa (mostly Mesozoic fossils, 66–252 Ma). In both analyses,
317 we focused on a common set of extant taxa to subset the full supermatrix for molecular
318 characters (59 mammals, representing each of the 28 patch clades plus select family-level taxa
319 with morphological data, and 1 outgroup *Anolis carolinensis*). ND and FBD analyses were
320 conducted in MrBayes analogously to patch clades, and compared to test dating sensitivity (*SI*
321 *Appendix*, Fig. S9, Table S6, Dataset S5).

322 **Construction of full dated mammalian phylogenies.** Tree distributions from the 28
323 patch subclades (TopoCons and TopoFree) and two backbones (ND and FBD) was performed in
324 ape (70), as outlined in the *SI Appendix*. Sets of 10,000 trees will be available in the phylogeny
325 subsetting tool at vertlife.org/phylosubsets and temporarily at XXXXXXX.

326 ***Tests for diversification-rate variation or constancy* -- Tip-level rates.** Following ref.
327 (11) we calculated per-species estimates of expected pure-birth (PB) diversification rates for the
328 instantaneous present moment (tips of the tree) using the inverse of the equal splits measure (11,
329 12). We call this metric 'tip-level diversification rate' (tip DR) because it measures recent
330 diversification processes among extant species (7) (≈ speciation rate, if recent extinction is
331 minimal (71)). Tip DR is tightly associated with more complex tip-level metrics (*SI Appendix*,
332 Fig. S4a), and as a clade-level harmonic mean approximates PB clade rates (R^2: ~0.7 versus ~0.5
333 for BD speciation and net diversification rates; *SI Appendix*, Fig. S4b).

334 **Lineage-specific rate shifts.** We performed searches for macroevolutionary shifts using
335 BAMM v2.5 (43), a reversible-jump algorithm for sampling birth-death scenarios of variable rate
336 regimes without a prior hypothesis. The high degree of phylogenetic uncertainty across our trees
337 (~30% completed species) prompted us to evaluate the number and location of rate shifts on 10

338 trees from the node-dated sample. We summarized across the most likely shifts per tree—called
339 maximum shift credibility (MSC) sets (*SI Appendix*, Fig. S15a)—using the ratio of the mean net
340 diversification rate of all branches inside the shifted clade (clade rate) and outside that clade
341 (background rate) to calculate the rate shift magnitude and direction for each MSC set (*SI*
342 *Appendix*, Table S8 and Dataset S7; for tree-wide rate shifts, see *SI Appendix*, Fig. S15-S16).

343 **Fossil diversification.** We analyzed Mammalia fossil occurrence data from the
344 Paleobiology Database (72), grouping by genus after excluding ichnotaxa and uncertain genera,
345 we recovered 71,928 occurrences of 5300 genera, which we binned in 10-Ma intervals and used
346 shareholder quorum subsampling (SQS (73); quorum size: 0.5) to maximize the uniformity of
347 coverage. Corresponding origination and extinction rates per stage were calculated using the per-
348 capita rate method (74), and the oldest fossil per extant order was compared to stem ages in our
349 node-dated phylogeny (*SI Appendix*, Fig. S13, Table S7).

350 **Likelihood tests of RC and RV models of diversification.** We analyzed the branching
351 times of 27 named subclades (11 orders and 16 suborders) that contained ≥25 species. For each
352 subclade, we tested 10 models developed by Morlon et al. (42): two rate-constant (RC) models,
353 constant PB and BD; and eight rate-variable (RV) models, with exponentially and linearly time-
354 varying rates. We fit models for 100 trees of the empirical subclades and their matching RC-
355 simulated trees (null models, simulated under the empirical extinction fractions of ~ ε=0.65 over
356 100 trees using the "pbtree" function in phytools (75)). Subtracting AICc scores of the best-
357 fitting RC and RV models provided the $\Delta AIC_{RC\text{-}RV}$ test statistic per tree and subclade for
358 comparison to the simulated null distribution (alpha=0.05; see *SI Appendix*, Table S9).

359 **Time-sliced clades and clade-level PGLS.** To objectively define clades, we arbitrarily
360 drew lines (referred to as "time slices") at 5-Ma intervals and took the resulting *tipward*
361 monophyletic clades as non-nested units of analysis. The *rootward* relationships of those clades
362 (the "rootward backbone") was retained for each interval, giving the expected covariance
363 structure among clades when performing phylogenetic generalized least squares (PGLS) analyses
364 (*SI Appendix*, Fig. S5 for illustration). We used the "treeSlice" function in phytools to construct
365 clade sets across Mammalia trees and the three sets of RC simulations, empirical (ε=0.65), low
366 (ε=0.2), and high (ε=0.8), also comparing our results to analyses on traditional taxon-based
367 clades (genera, families, and orders; *SI Appendix*, Fig. S18-S20). All PGLS was performed
368 excluding extinct species, using Pagel's "lambda" transformation in phylolm (optimized for large
369 trees (76)), and repeating the analysis across 100 or 1000 trees.

370 ***Tests for causes of diversification-rate variation* -- Mammalian trait data.** Our
371 workflow for gathering trait data involved (i) unifying multiple trait taxonomies (e.g.,
372 EltonTraits v1.0 (77)) to our phylogeny's master taxonomy; and (ii) interpolating home range
373 area and vagility to the species level using known allometric relationships in mammals (*SI*
374 *Appendix*, Fig. S6, Dataset S7). Vagility was calculated as the maximum natal dispersal distance
375 per individual (km) and interpolated for each species following our updated version of Whitmee
376 and Orme's (78) best-fit equation, testing for collinearity prior to analyses (*SI Appendix*, Fig.
377 S7).

378 **Tip-level correlates of diversification rates.** To better understand correlative structures
379 underlying the observed rate variation, we performed tip-level PGLS analyses between species'
380 ecological traits and tip DR values across 1000 trees, focusing on a 5675-species data set that
381 excluded all extinct (n=107) and marine (n=129) species. We followed Freckleton et al. (8) in

using trait ~ rate models in our tip-level PGLS analyses to avoid identical residuals in the dependent variable (i.e., sister species have identical tip DR values, violating the assumption of within-variable data independence in bivariate normal distributions). The trait ~ rate approach has been applied using tip DR in univariate contexts (79) (see *SI Appendix*, Fig. S21 for sensitivity tests).

Clade-level correlates of diversification rates. At the clade level, univariate PGLS was performed typically (rate ~ trait models), since clade tip DR mean gave independent values to sister clades. These analyses were conducted on 1000 trees by analogy with those previous, except that per-clade trait summaries were the standardized predictors (geometric means for vagility, otherwise arithmetic means). We also performed tests for trait-dependent diversification using rate-shifted clades identified in BAMM runs on 10 mammal trees (STRAPP (80) method), which corrects for phylogenetic pseudoreplication similar to PGLS except considering only the covariance structure among rate regimes (see *SI Appendix*, Fig. S17).

Phylogenetic path analyses. Path analysis aims to fully resolve correlational structures and thereby translate from the language of statistical probability to causality. In phylogenetic path analyses, we used PGLS to test statements of conditional independence (53) across 27 pre-selected path models (*SI Appendix*, Fig. S8). For each tree and clade set, we used "phylopath" (81) to analyze models and perform conditional model averaging. Time-sliced clades at 10-, 30-, and 50-Ma intervals were analyzed along with taxon-based clades (*SI Appendix*, Fig. S20, S22).

Data availability. All data and code is available in the manuscript, supplementary materials, and after publication on Dryad (all code will be available at github.com/n8upham/).

Acknowledgments

We thank I. Quintero, M. Landis, D. Schluter, A. Mooers, A. Pyron, G. Thomas, D. Greenberg, and E. Florsheim for conceptual discussions that improved this study; B. Patterson, K. Rowe, J. Brown, T. Colston, T. Peterson, D. Field, T. Stewart, J. Davies, and three anonymous reviewers for comments on earlier drafts; S. Upham for improving figure design; C. Meyer for his synonym list; and M. Koo, A. Ranipeta, J. Hart, M. Swanson, C. Burgin, and J. Colella for database help. Artwork from phylopic.org and open source fonts. The NSF VertLife Terrestrial grant to W.J. and J.E. (DEB 1441737 and 1441634) and NSF grant DBI-1262600 to W.J. supported this work.

References

1. Willis JC (1922) *Age and Area* (Cambridge University Press, Cambridge).
2. Mooers AO, Heard SB (1997) Inferring Evolutionary Process from Phylogenetic Tree Shape. *Q Rev Biol* 72(1):31–54.
3. Mittelbach GG, et al. (2007) Evolution and the latitudinal diversity gradient: speciation, extinction and biogeography. *Ecol Lett* 10(4):315–331.
4. Rabosky DL, Slater GJ, Alfaro ME (2012) Clade age and species richness are decoupled across the eukaryotic tree of life. *PLoS Biol* 10:e1001381.
5. Purvis A, Fritz SA, Rodríguez J, Harvey PH, Grenyer R (2011) The shape of mammalian phylogeny: patterns, processes and scales. *Philos Trans R Soc Lond B Biol Sci* 366(1577):2462–2477.
6. Simpson GG (1953) *The major features of evolution* (Columbia Univ Press, New York).
7. Quintero I, Jetz W (2018) Global elevational diversity and diversification of birds. *Nature*.
8. Freckleton RP, Phillimore AB, Pagel M (2008) Relating Traits to Diversification: A Simple Test. *Am Nat* 172(1):102–115.
9. Jablonski D (2008) Species Selection: Theory and Data. *Annu Rev Ecol Evol Syst* 39(1):501–524.
10. Rabosky DL (2014) Automatic Detection of Key Innovations, Rate Shifts, and Diversity-Dependence on Phylogenetic Trees. *PLOS ONE* 9(2):e89543.
11. Jetz W, Thomas GH, Joy JB, Hartmann K, Mooers AO (2012) The global diversity of birds in space and time. *Nature* 491(7424):444–448.
12. Steel M, Mooers A (2010) The expected length of pendant and interior edges of a Yule tree. *Appl Math Lett* 23(11):1315–1319.
13. Schluter D, Pennell MW (2017) Speciation gradients and the distribution of biodiversity. *Nature* 546(7656):48–55.
14. Weir JT, Schluter D (2007) The Latitudinal Gradient in Recent Speciation and Extinction Rates of Birds and Mammals. *Science* 315(5818):1574–1576.
15. Rabosky DL, et al. (2018) An inverse latitudinal gradient in speciation rate for marine fishes. *Nature*:1.
16. Rosenblum EB, et al. (2012) Goldilocks Meets Santa Rosalia: An Ephemeral Speciation Model Explains Patterns of Diversification Across Time Scales. *Evol Biol* 39(2):255–261.
17. Yoder JB, et al. (2010) Ecological opportunity and the origin of adaptive radiations. *J Evol Biol* 23:1581–1596.
18. Schluter D (2000) *The ecology of adaptive radiation* (Oxford University Press, Oxford, UK).
19. Mayr E (1963) *Animal species and evolution* (Belknap, Cambridge, MA).
20. Jablonski D (1986) Larval ecology and macroevolution in marine invertebrates. *Bull Mar Sci* 39(2):565–587.
21. Claramunt S, Derryberry EP, Remsen JV, Brumfield RT (2012) High dispersal ability inhibits speciation in a continental radiation of passerine birds. *Proc R Soc Lond B Biol Sci* 279(1733):1567–1574.
22. Bininda-Emonds ORP (2004) The evolution of supertrees. *Trends Ecol Evol* 19(6):315–322.
23. Bininda-Emonds ORP, et al. (2007) The delayed rise of present-day mammals. *Nature* 446(7135):507–512.
24. Fritz SA, Bininda-Emonds ORP, Purvis A (2009) Geographical variation in predictors of mammalian extinction risk: big is bad, but only in the tropics. *Ecol Lett* 12(6):538–549.

25. Kuhn TS, Mooers AØ, Thomas GH (2011) A simple polytomy resolver for dated phylogenies. *Methods Ecol Evol* 2(5):427–436.
26. Stadler T (2011) Mammalian phylogeny reveals recent diversification rate shifts. *Proc Natl Acad Sci* 108(15):6187–6192.
27. Faurby S, Svenning J-C (2015) A species-level phylogeny of all extant and late Quaternary extinct mammals using a novel heuristic-hierarchical Bayesian approach. *Mol Phylogenet Evol* 84:14–26.
28. Hedges SB, Marin J, Suleski M, Paymer M, Kumar S (2015) Tree of life reveals clock-like speciation and diversification. *Mol Biol Evol*:msv037.
29. Tonini JFR, Beard KH, Ferreira RB, Jetz W, Pyron RA (2016) Fully-sampled phylogenies of squamates reveal evolutionary patterns in threat status. *Biol Conserv* 204:23–31.
30. Jetz W, Pyron RA (2018) The interplay of past diversification and evolutionary isolation with present imperilment across the amphibian tree of life. *Nat Ecol Evol*.
31. Benton MJ, et al. (2015) Constraints on the timescale of animal evolutionary history. *Palaeontol Electron* 18(1).
32. Zhou C-F, Wu S, Martin T, Luo Z-X (2013) A Jurassic mammaliaform and the earliest mammalian evolutionary adaptations. *Nature* 500(7461):163–167.
33. Nee S, May RH, Harvey PH (1994) The reconstructed evolutionary process. *Philos Trans R Soc Lond B-Biol Sci* 344:305–311.
34. Nee S, May RM (1997) Extinction and the Loss of Evolutionary History. *Science* 278(5338):692–694.
35. Meredith RW, et al. (2011) Impacts of the Cretaceous Terrestrial Revolution and KPg Extinction on Mammal Diversification. *Science* 334(6055):521–524.
36. Archibald JD, Deutschman DH (2001) Quantitative Analysis of the Timing of the Origin and Diversification of Extant Placental Orders. *J Mamm Evol* 8(2):107–124.
37. dos Reis M, et al. (2012) Phylogenomic datasets provide both precision and accuracy in estimating the timescale of placental mammal phylogeny. *Proc R Soc Lond B Biol Sci* 279(1742):3491–3500.
38. Grossnickle DM, Newham E (2016) Therian mammals experience an ecomorphological radiation during the Late Cretaceous and selective extinction at the K–Pg boundary. *Proc R Soc B* 283(1832):20160256.
39. Pires MM, Rankin BD, Silvestro D, Quental TB (2018) Diversification dynamics of mammalian clades during the K–Pg mass extinction. *Biol Lett* 14(9):20180458.
40. Kalmar A, Currie DJ (2010) The Completeness of the Continental Fossil Record and Its Impact on Patterns of Diversification. *Paleobiology* 36(1):51–60.
41. Alroy J (1999) The Fossil Record of North American Mammals: Evidence for a Paleocene Evolutionary Radiation. *Syst Biol* 48(1):107–118.
42. Morlon H, Parsons TL, Plotkin JB (2011) Reconciling molecular phylogenies with the fossil record. *Proc Natl Acad Sci* 108(39):16327–16332.
43. Rabosky DL (2014) Automatic detection of key innovations, rate shifts, and diversity-dependence on phylogenetic trees. *PLoS ONE* 9:e89543.
44. Katz ME, et al. (2008) Stepwise transition from the Eocene greenhouse to the Oligocene icehouse. *Nat Geosci* 1(5):329–334.
45. Venditti C, Meade A, Pagel M (2011) Multiple routes to mammalian diversity. *Nature* 479(7373):393–396.

46. Ricklefs RE (2003) Global diversification rates of passerine birds. *Proc R Soc Lond B-Biol Sci* 270:2285–2291.
47. Price TD (2010) The roles of time and ecology in the continental radiation of the Old World leaf warblers (*Phylloscopus* and *Seicercus*). *Philos Trans R Soc Lond B Biol Sci* 365(1547):1749–1762.
48. Nee S, Holmes EC, May RM, Harvey PH (1994) Extinction rates can be estimated from molecular phylogenies. *Philos Trans R Soc Lond B-Biol Sci* 344:77–82.
49. Venditti C, Meade A, Pagel M (2010) Phylogenies reveal new interpretation of speciation and the Red Queen. *Nature* 463(7279):349–352.
50. Gerkema MP, Davies WIL, Foster RG, Menaker M, Hut RA (2013) The nocturnal bottleneck and the evolution of activity patterns in mammals. *Proc R Soc B* 280(1765):20130508.
51. Kisel Y, Barraclough TG (2010) Speciation Has a Spatial Scale That Depends on Levels of Gene Flow. *Am Nat* 175(3):316–334.
52. Jablonski D (1987) Heritability at the Species Level: Analysis of Geographic Ranges of Cretaceous Mollusks. *Science* 238(4825):360–363.
53. von Hardenberg A, Gonzalez-Voyer A (2013) Disentangling Evolutionary Cause-Effect Relationships with Phylogenetic Confirmatory Path Analysis. *Evolution* 67(2):378–387.
54. Hewitt G (2000) The genetic legacy of the Quaternary ice ages. *Nature* 405(6789):907–913.
55. Marcot JD, Fox DL, Niebuhr SR (2016) Late Cenozoic onset of the latitudinal diversity gradient of North American mammals. *Proc Natl Acad Sci* 113(26):7189–7194.
56. Maor R, Dayan T, Ferguson-Gow H, Jones KE (2017) Temporal niche expansion in mammals from a nocturnal ancestor after dinosaur extinction. *Nat Ecol Evol* 1(12):1889.
57. Arbour JH, Santana SE (2017) A major shift in diversification rate helps explain macroevolutionary patterns in primate species diversity. *Evolution* 71(6):1600–1613.
58. Thomas GH, et al. (2013) PASTIS: an R package to facilitate phylogenetic assembly with soft taxonomic inferences. *Methods Ecol Evol* 4(11):1011–1017.
59. Altschul SF, et al. (1997) Gapped BLAST and PSI-BLAST: a new generation of protein database search programs. *Nucleic Acids Res* 25:3389–3402.
60. Wilson DE, Reeder DM (2005) *Mammal species of the world: a taxonomic and geographic reference, 3rd ed.* (Johns Hopkins University Press, Baltimore, MD). 3rd Ed.
61. Meyer C, Kreft H, Guralnick R, Jetz W (2015) Global priorities for an effective information basis of biodiversity distributions. *Nat Commun* 6:8221.
62. Burgin CJ, Colella JP, Kahn PL, Upham NS (2018) How many species of mammals are there? *J Mammal* 99(1):1–14.
63. Mammal Diversity Database (2018) American Society of Mammalogists, Mammal Diversity Database. Available at: https://mammaldiversity.org/ [Accessed June 2, 2018].
64. Stamatakis A (2014) RAxML version 8: a tool for phylogenetic analysis and post-analysis of large phylogenies. *Bioinformatics* 30(9):1312–1313.
65. Wiens JJ, Morrill MC (2011) Missing Data in Phylogenetic Analysis: Reconciling Results from Simulations and Empirical Data. *Syst Biol*:syr025.
66. Roure B, Baurain D, Philippe H (2013) Impact of Missing Data on Phylogenies Inferred from Empirical Phylogenomic Data Sets. *Mol Biol Evol* 30(1):197–214.
67. Ronquist F, et al. (2012) MrBayes 3.2: Efficient Bayesian Phylogenetic Inference and Model Choice across a Large Model Space. *Syst Biol*:sys029.
68. Phillips MJ (2015) Four mammal fossil calibrations: balancing competing palaeontological and molecular considerations. *Palaeontol Electron* 18(1):1–16.

69. Heath TA, Huelsenbeck JP, Stadler T (2014) The fossilized birth–death process for coherent calibration of divergence-time estimates. *Proc Natl Acad Sci* 111(29):E2957–E2966.
70. Paradis E, Claude J, Strimmer K (2004) APE: Analyses of Phylogenetics and Evolution in R language. *Bioinformatics* 20:289–290.
71. Title PO, Rabosky D (2018) Tip rates, phylogenies and diversification: what are we estimating, and how good are the estimates? *bioRxiv*:369124.
72. Alroy J, et al. (2018) Taxonomic occurrences of Mammalia recorded in Fossilworks, the Evolution of Terrestrial Ecosystems database, and the Paleobiology Database. Fossilworks. http://fossilworks.org.
73. Alroy J (2014) Accurate and precise estimates of origination and extinction rates. *Paleobiology* 40(3):374–397.
74. Foote M (2000) Origination and extinction components of taxonomic diversity: general problems. *Paleobiology* 26(sp4):74–102.
75. Revell LJ (2012) phytools: an R package for phylogenetic comparative biology (and other things). *Methods Ecol Evol* 3:217–223.
76. Ho LST, Ané C (2014) A Linear-Time Algorithm for Gaussian and Non-Gaussian Trait Evolution Models. *Syst Biol* 63(3):397–408.
77. Wilman H, et al. (2014) EltonTraits 1.0: Species-level foraging attributes of the world's birds and mammals. *Ecology* 95(7):2027–2027.
78. Whitmee S, Orme CDL (2013) Predicting dispersal distance in mammals: a trait-based approach. *J Anim Ecol* 82(1):211–221.
79. Harvey MG, et al. (2017) Positive association between population genetic differentiation and speciation rates in New World birds. *Proc Natl Acad Sci* 114(24):6328–6333.
80. Rabosky DL, Huang H (2016) A Robust Semi-Parametric Test for Detecting Trait-Dependent Diversification. *Syst Biol* 65(2):181–193.
81. van der Bijl W (2018) phylopath: Easy phylogenetic path analysis in R. *PeerJ* 6:e4718.

576 **Figure legends**

577 **Fig. 1. Species-level relationships and diversification rates across mammals.** The node-dated
578 analysis of 5911 species shows branches colored with tip-level diversification rates (tip DR) and
579 marked with 24 shifts in lineage diversification rates (labels A-X; shifts with multiple circles
580 occurred on either branch, not both; all shifts were detected in ≥ 5 of 10 trees analyzed in
581 BAMM (43)). Maximum clade credibility topology of 10,000 trees. Numbered clade labels
582 correspond to orders and subclades listed in the plot periphery: Mars, Marsupialia; X, Xenarthra;
583 Afro, Afrotheria; Laur, Laurasiatheria; Euar, Euarchontoglires. Scale in millions of years, Ma.

584 **Fig. 2. Building the backbone-and-patch Mammalia phylogenies.** (a) Schematic overview of
585 DNA sequence gathering from NCBI, taxonomic matchup, iterative error checking, and
586 estimating a global maximum-likelihood (ML) tree from the resulting supermatrix (31 genes by
587 4098 species (64)). Subclade (patch) phylogenies were then delimited, estimated using Bayesian
588 inference (67), and joined to fossil-calibrated backbone trees (node- or tip-dated). The resulting
589 posterior samples of 10,000 fully dated phylogenies either had the global ML tree topology
590 constrained (completed trees of 5911 species, 'TopoCons') or no topology constraints (DNA-
591 only trees, 'TopoFree'). (b) Backbone trees contained topological and age uncertainty, including
592 the unresolved base of Placentalia (e.g., (35)), slightly favoring the Atlantogenata hypothesis
593 (blue) versus Exafroplacentalia (red). (c) Bayesian phylogenies of 28 patch clades were
594 separately estimated in relative-time units for re-scaling to representative divergence times on the
595 backbone. Combining sets of backbones and patch clades yielded four posterior distributions for
596 analysis (see *SI Appendix*, Fig. S9-12).

597 **Fig. 3. Diversification rate variation among mammal clades.** Lineage-through-time plots and
598 estimated crown ages for (**a**) all superordinal divergences, and (**b**) placental orders with crown
599 age estimates overlapping the Cretaceous-Paleogene extinction event (K-Pg, dashed gray line;
600 means and 95% CIs; filled circle if statistically different). (**c**) Rate-through-time plots for
601 speciation, extinction, and net diversification (summarized from Fig. 1 rate shifts; medians from
602 10 trees, 95% CIs in light gray). (**d**) Fossil genus diversity through time for all Mammalia,
603 including subsampled genus richness (quorum 0.5) and per-capita rates of genus origination and
604 extinction. (**e**) Extant rates and lineage-specific rate shifts for the five most speciose mammal
605 orders (same symbols as in **c**). (**f**) Rate variation within subclades of these five orders as
606 numbered from Fig. 1; left: difference in AIC between best-fit models of diversification for trees
607 simulated under rate-constant birth-death (gray) versus observed mammal trees (color; filled
608 circle and * if ΔAIC on 100 trees is statistically different); and, right: tip DR distributions of the
609 same simulated and observed subclades (gray versus color, one tree), comparing variation in tip
610 DR mean and skew across 100 trees. The last 2 Ma are removed from parts **c-e** for clarity.

611 **Fig. 4. Age and rate components of species richness variation across time-slice defined**
612 **clades. (a)** The log species richness of clades tipward of each 5-Ma time slice (dotted lines from
613 5-70 Ma) across a sample of 100 phylogenies (maximum clade credibility tree shown) is best
614 predicted jointly by (**b**) clade crown age, (**c**) clade tip DR mean, and (**d**) clade tip DR skew.
615 Multivariate phylogenetic analyses of clade richness in observed trees (gray) is compared to trees
616 simulated under rate-constant birth and death with different extinction fractions, ε (colors in
617 legend; PGLS on standardized data with 95% confidence intervals [CIs] on parameter estimates).
618 Solid black lines are the observed best-fitting models given random effects of time slice and tree.
619 Insets (**b** to **d**) are examples from 35-Ma clades (red line) showing the bivariate plots underlying
620 each multivariate PGLS slope per tree and time slice.

621 **Fig. 5. Ecological drivers of (a) species diversification and (b) clade diversification and**
622 **richness.** (**a**, top panel) Distribution of species-level diversification rates (tip DR, mean of
623 10,000 trees) relative to per-species estimates of vagility (maximum natal dispersal distance),
624 diurnality (0=nocturnal or cathemeral, 1=diurnal), and absolute value of latitude (centroid of
625 expert maps) across 5,675 species (excluding extinct and marine species). Loess smoothing lines
626 visualize general trends (blue, span=0.33). Species-level effects (bottom panel) from univariate
627 PGLS between tip DR and ecological traits subset across trophic levels (1000 trees, 95% CI,
628 colored if significant). (**b**) Phylogenetic path analysis (53) of putative causal relationships
629 between traits and rates leading to clade species richness for time-sliced clades. Path thickness,
630 color, and directionality denote median coefficients of model-averaged analyses. The bottom
631 panels provide per-estimate uncertainty across time slices (slope ± SE, 1000 trees). Non-zero
632 estimates, either positive (blue shades) or negative (red shades), are totaled in the right margin;
633 paths present in >500 trees are bolded and displayed in path model whereas others are dashed.

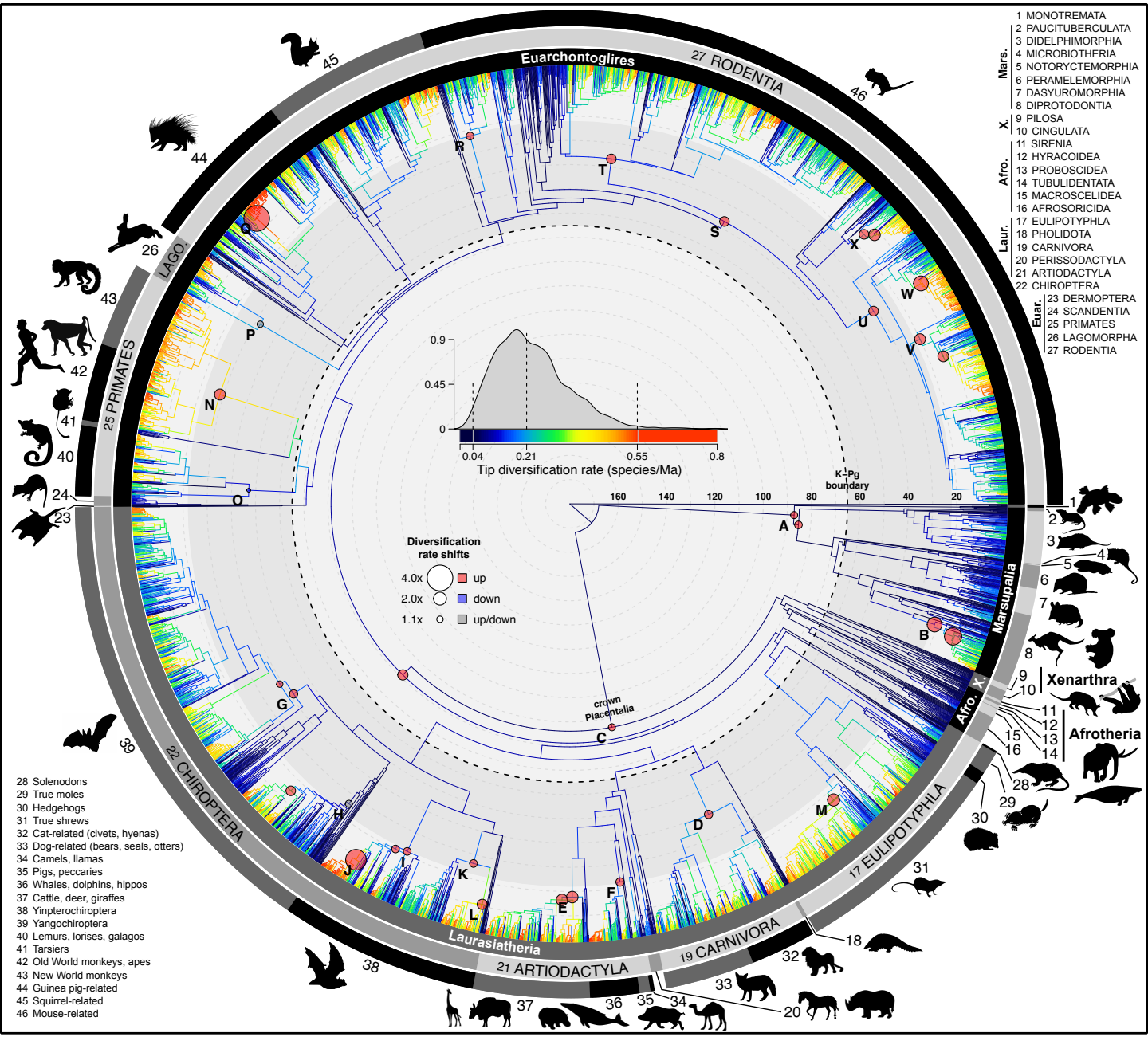
Euarchontoglires
27 RODENTIA
46
45
44
26
LAGO.
43
42
41
40
25 PRIMATES
24
23
39
22 CHIROPTERA
38
37
36
35
34
20
21 ARTIODACTYLA
19 CARNIVORA
33
32
18
17 EULIPOTYPHLA
31
30
29
28
Afro.
X.
Xenarthra
Afrotheria
Marsupalia
1
2
3
4
5
6
7
8
9
10
11
12
13
14
15
16
Laurasiatheria
0.9
0.45
0
0.04
0.21
0.55
0.8
Tip diversification rate (species/Ma)
K–Pg boundary
160
140
120
100
80
60
40
20
crown Placentalia
Diversification rate shifts
4.0x
2.0x
1.1x
up
down
up/down
A
B
C
D
E
F
G
H
I
J
K
L
M
N
O
P
Q
R
S
T
U
V
W
X
Mars.
X.
Afro.
Laur.
Euar.
1 MONOTREMATA
2 PAUCITUBERCULATA
3 DIDELPHIMORPHIA
4 MICROBIOTHERIA
5 NOTORYCTEMORPHIA
6 PERAMELEMORPHIA
7 DASYUROMORPHIA
8 DIPROTODONTIA
9 PILOSA
10 CINGULATA
11 SIRENIA
12 HYRACOIDEA
13 PROBOSCIDEA
14 TUBULIDENTATA
15 MACROSCELIDEA
16 AFROSORICIDA
17 EULIPOTYPHLA
18 PHOLIDOTA
19 CARNIVORA
20 PERISSODACTYLA
21 ARTIODACTYLA
22 CHIROPTERA
23 DERMOPTERA
24 SCANDENTIA
25 PRIMATES
26 LAGOMORPHA
27 RODENTIA
28 Solenodons
29 True moles
30 Hedgehogs
31 True shrews
32 Cat-related (civets, hyenas)
33 Dog-related (bears, seals, otters)
34 Camels, llamas
35 Pigs, peccaries
36 Whales, dolphins, hippos
37 Cattle, deer, giraffes
38 Yinpterochiroptera
39 Yangochiroptera
40 Lemurs, lorises, galagos
41 Tarsiers
42 Old World monkeys, apes
43 New World monkeys
44 Guinea pig-related
45 Squirrel-related
46 Mouse-related

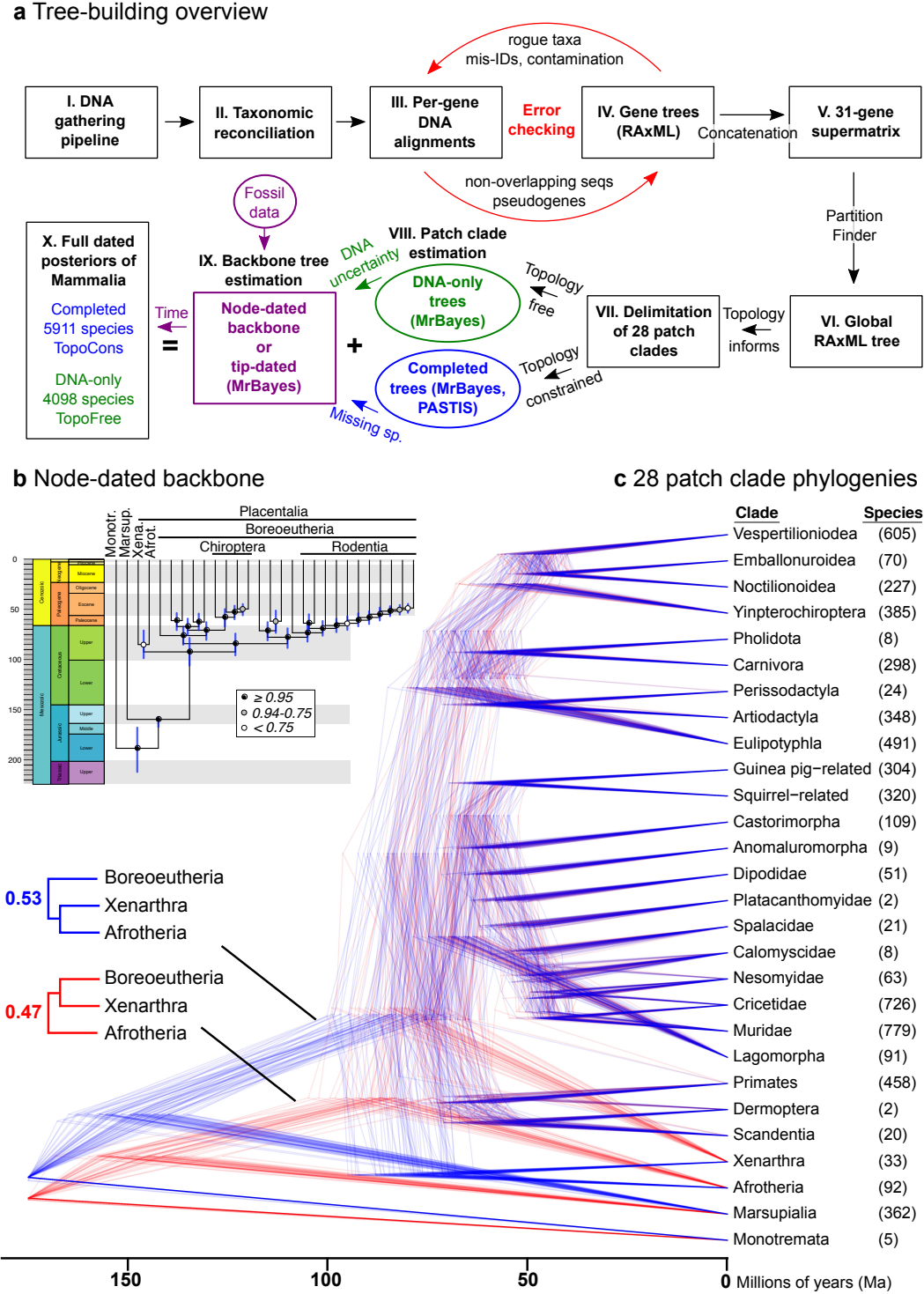
a Tree-building overview
rogue taxa
mis-IDs, contamination
I. DNA gathering pipeline
II. Taxonomic reconciliation
III. Per-gene DNA alignments
Error checking
IV. Gene trees (RAxML)
Concatenation
V. 31-gene supermatrix
non-overlapping seqs
pseudogenes
Partition Finder
Fossil data
X. Full dated posteriors of Mammalia
Completed 5911 species TopoCons
DNA-only 4098 species TopoFree
Time
=
IX. Backbone tree estimation
Node-dated backbone or tip-dated (MrBayes)
+
DNA uncertainty
VIII. Patch clade estimation
DNA-only trees (MrBayes)
Topology free
Completed trees (MrBayes, PASTIS)
Topology constrained
Missing sp.
VII. Delimitation of 28 patch clades
Topology informs
VI. Global RAxML tree
b Node-dated backbone
Monotr.
Marsup.
Xena.
Afrot.
Placentalia
Boreoeutheria
Chiroptera
Rodentia
Cenozoic
Mesozoic
Paleogene
Neogene
Cretaceous
Jurassic
Triassic
Miocene
Oligocene
Eocene
Paleocene
Upper
Lower
Middle
0
50
100
150
200
≥ 0.95
0.94-0.75
< 0.75
0.53
Boreoeutheria
Xenarthra
Afrotheria
0.47
Boreoeutheria
Xenarthra
Afrotheria
c 28 patch clade phylogenies
Clade
Species
Vespertilionioidea (605)
Emballonuroidea (70)
Noctilionoidea (227)
Yinpterochiroptera (385)
Pholidota (8)
Carnivora (298)
Perissodactyla (24)
Artiodactyla (348)
Eulipotyphla (491)
Guinea pig−related (304)
Squirrel−related (320)
Castorimorpha (109)
Anomaluromorpha (9)
Dipodidae (51)
Platacanthomyidae (2)
Spalacidae (21)
Calomyscidae (8)
Nesomyidae (63)
Cricetidae (726)
Muridae (779)
Lagomorpha (91)
Primates (458)
Dermoptera (2)
Scandentia (20)
Xenarthra (33)
Afrotheria (92)
Marsupialia (362)
Monotremata (5)
150
100
50
0
Millions of years (Ma)

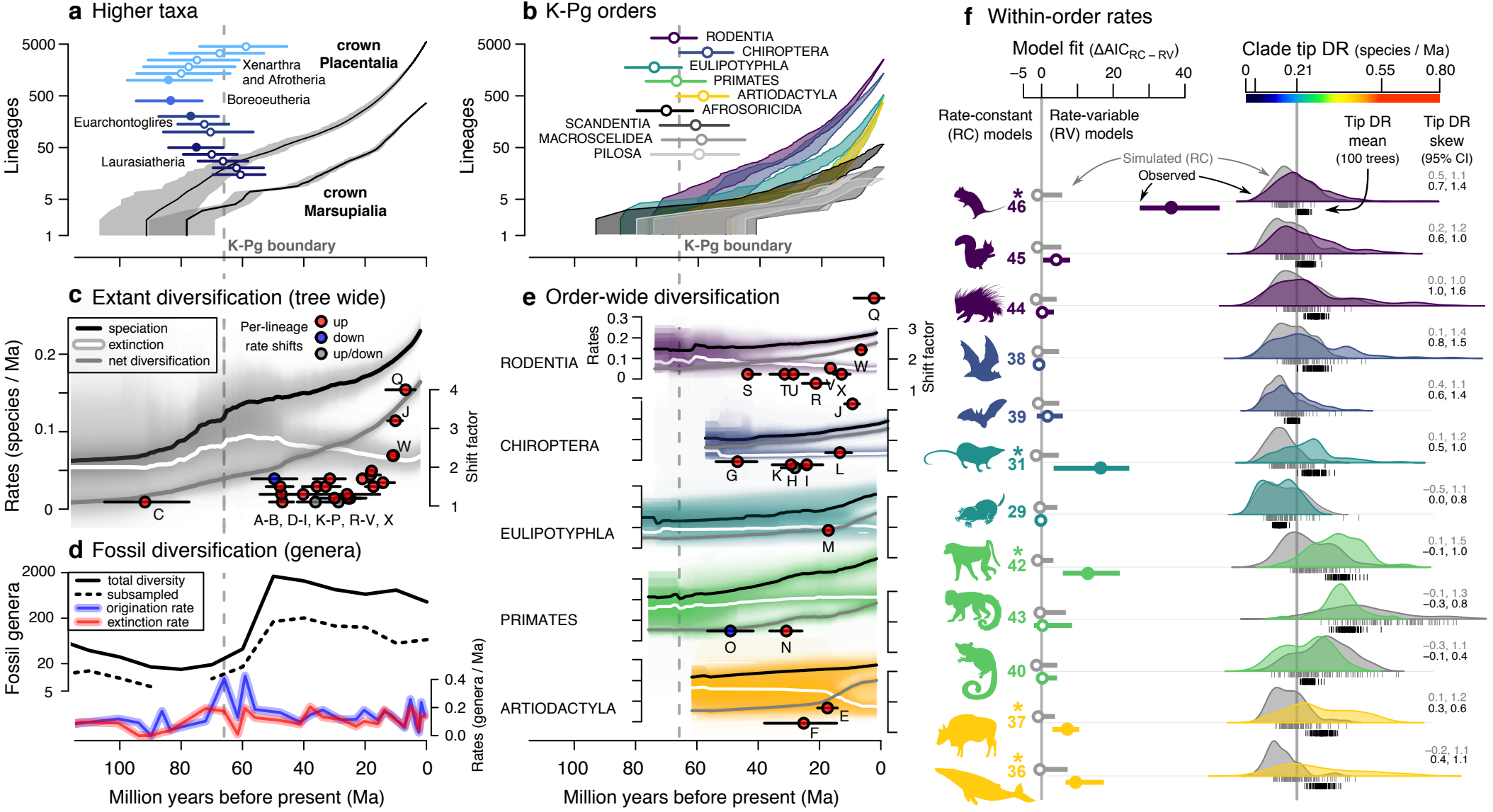
a Higher taxa
Lineages
5000
500
50
5
1
crown Placentalia
Xenarthra and Afrotheria
Boreoeutheria
Euarchontoglires
Laurasiatheria
crown Marsupialia
K-Pg boundary
b K-Pg orders
RODENTIA
CHIROPTERA
EULIPOTYPHLA
PRIMATES
ARTIODACTYLA
AFROSORICIDA
SCANDENTIA
MACROSCELIDEA
PILOSA
c Extant diversification (tree wide)
speciation
extinction
net diversification
Per-lineage rate shifts
up
down
up/down
Rates (species / Ma)
Shift factor
A-B, D-I, K-P, R-V, X
d Fossil diversification (genera)
total diversity
subsampled
origination rate
extinction rate
Fossil genera
Rates (genera / Ma)
Million years before present (Ma)
e Order-wide diversification
Rates
Shift factor
Million years before present (Ma)
f Within-order rates
Model fit (ΔAIC RC – RV)
Clade tip DR (species / Ma)
Rate-constant (RC) models
Rate-variable (RV) models
Simulated (RC)
Observed
Tip DR mean (100 trees)
Tip DR skew (95% CI)
46
45
44
38
39
31
29
42
43
40
37
36

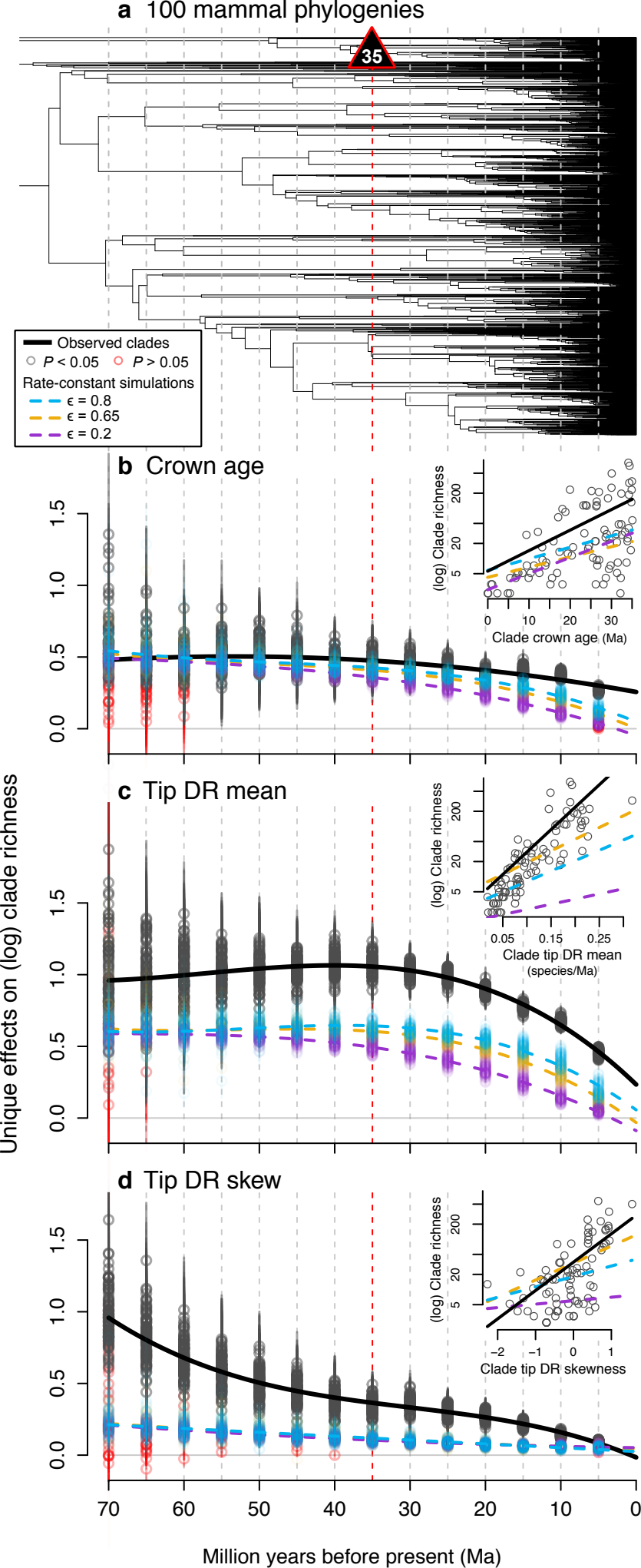
a 100 mammal phylogenies
35
Observed clades
P < 0.05
P > 0.05
Rate-constant simulations
ϵ = 0.8
ϵ = 0.65
ϵ = 0.2
b Crown age
(log) Clade richness
Clade crown age (Ma)
c Tip DR mean
Clade tip DR mean (species/Ma)
d Tip DR skew
Clade tip DR skewness
Unique effects on (log) clade richness
Million years before present (Ma)

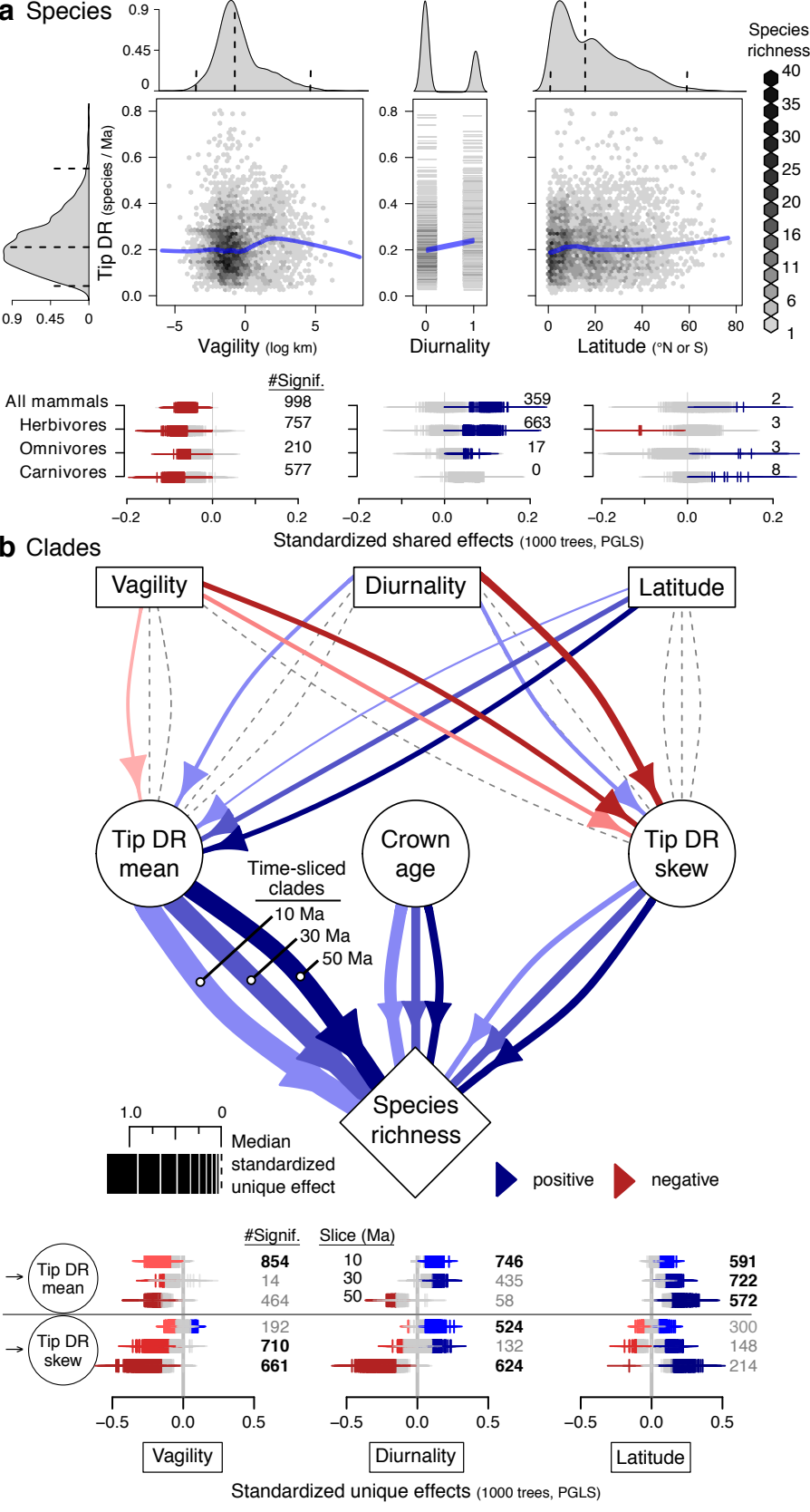
a Species
Species richness
Tip DR (species / Ma)
Vagility (log km)
Diurnality
Latitude (°N or S)
#Signif.
All mammals
Herbivores
Omnivores
Carnivores
998
757
210
577
359
663
17
0
2
3
3
8
Standardized shared effects (1000 trees, PGLS)
b Clades
Vagility
Diurnality
Latitude
Tip DR mean
Crown age
Tip DR skew
Time-sliced clades
10 Ma
30 Ma
50 Ma
Species richness
Median standardized unique effect
positive
negative
#Signif.
Slice (Ma)
Tip DR mean
Tip DR skew
854
14
464
192
710
661
10
30
50
746
435
58
524
132
624
591
722
572
300
148
214
Vagility
Diurnality
Latitude
Standardized unique effects (1000 trees, PGLS)